INSTITUTE OF PHYSICS PUBLISHING PHYSICS IN MEDICINE AND BIOLOGY

Phys. Med. Biol. **50** (2005) 5203–5215 doi:10.1088/0031-9155/50/21/017

Response, thermal regulatory threshold and thermal breakdown threshold of restrained RF-exposed mice at 905 MHz

S Ebert[1,2], S J Eom[1,2], J Schuderer[2], U Apostel[3], T Tillmann[3], C Dasenbrock[3] and N Kuster[1,2]

[1] Swiss Federal Institute of Technology (ETH), Zurich, 8092 Zurich, Switzerland
[2] Foundation for Research on Information Technologies in Society (IT'IS), Zeughausstrasse 43, 8004 Zurich, Switzerland
[3] Fraunhofer Institute for Toxicology and Experimental Medicine, Nicolai-Fuchs-Strasse 1, 30625 Hannover, Germany

E-mail: ebert@itis.ethz.ch

Received 22 January 2005, in final form 26 July 2005
Published 20 October 2005
Online at stacks.iop.org/PMB/50/5203

Abstract

The objective of this study was the determination of the thermal regulatory and the thermal breakdown thresholds for in-tube restrained B6C3F1 and NMRI mice exposed to radiofrequency electromagnetic fields at 905 MHz. Different levels of the whole-body averaged specific absorption rate (SAR = 0, 2, 5, 7.2, 10, 12.6 and 20 W kg^{-1}) have been applied to the mice inside the 'Ferris Wheel' exposure setup at 22 ± 2 °C and 30–70% humidity. The thermal responses were assessed by measurement of the rectal temperature prior, during and after the 2 h exposure session. For B6C3F1 mice, the thermal response was examined for three different weight groups (20 g, 24 g, 29 g), both genders and for pregnant mice. Additionally, NMRI mice with a weight of 36 g were investigated for an interstrain comparison. The thermal regulatory threshold of in-tube restrained mice was found at SAR levels between 2 W kg^{-1} and 5 W kg^{-1}, whereas the breakdown of regulation was determined at 10.1 ± 4.0 W kg^{-1}($K = 2$) for B6C3F1 mice and 7.7 ± 1.6 W kg^{-1}($K = 2$) for NMRI mice. Based on a simplified power balance equation, the thresholds show a clear dependence upon the metabolic rate and weight. NMRI mice were more sensitive to thermal stress and respond at lower SAR values with regulation and breakdown. The presented data suggest that the thermal breakdown for in-tube restrained mice, whole-body exposed to radiofrequency fields, may occur at SAR levels of 6 W kg^{-1}($K = 2$) at laboratory conditions.

1. Introduction

Risk assessment studies examining the potential hazards of radiofrequency (RF) electromagnetic fields (EMF) focus on the question of whether the postulated EMF interactions below the thermal threshold may pose a health risk. These studies are faced with the methodological challenges that the thermal effects will occur shortly above local exposure levels, as they occur during everyday usage of, e.g., a mobile phone, so that the sensitivity towards EMF cannot be enhanced by applying a substantially increased dose. To maximize potentially risk relevant effects, studies are preferably performed just below the thermal threshold levels. This poses high requirements on the experimental exposure conditions (Kuster and Schonborn 2000); the exposure setup must deliver a well-defined dose with minimal variations in the applied EMF dose, and this also requires that the threshold levels must be carefully assessed.

The following power balance equation, in analogy to the heat balance equation formulated by Adair and Black (2003), is useful to discuss thermal response:

$$M + P_{\mathrm{RF}} - C = S. \tag{1}$$

Hereby M is the rate at which thermal energy is produced through metabolic processes, P_{RF} is the absorbed RF power, C is the cooling rate determined by the heat exchange via convection, radiation and evaporation and S is the rate of heat storage in the body. All units are expressed in Watts.

When mice are exposed to a heat load, e.g. from an increase in RF exposure, their initial main response is to linearly lower their metabolic rate in favour of stabilizing their body temperature (Adair *et al* 1992, 1993). When they reach their basal metabolic rate, other cooling mechanisms become dominant, such as an increase in evaporation (Gordon and White 1982), increase of skin temperature through vasolidation (Gordon 1983a) and behavioural changes (Gordon 1983b), such as spreading saliva or urine on their fur, or, if possible, choosing a new environment (Gordon 1982).

Three regions of thermal response to RF are distinguished in this paper: (1) a non-thermal regulatory region, where no measurable temperature response occurs, (2) a thermal regulatory region, where the regulatory system is able to compensate the absorbed energy and regulates to achieve a stable body temperature and (3) a thermal breakdown region, where the organism is not able to compensate the temperature increase. The thermal response regions are separated by two thresholds: the thermal regulatory threshold and the thermal breakdown threshold. Strictly defined, a thermal response may also occur without leading to measurable body temperature changes, e.g. as soon as a single thermal receptor detects a subtle temperature change and leads to cellular responses. However, such effects cannot be investigated by simple body temperature measurement and are therefore not the subject of this study.

Most of the published research on thermophysiological responses due to whole-body exposure to RF fields has been conducted with rodents (e.g. mice, rats and hamsters) (Gordon 1985a). However, no clear separation between thermal regulation and breakdown was targeted. A measurable thermal response in rodents was reported for SAR levels at various levels between 2 W kg^{-1} and 40 W kg^{-1} (Lu *et al* 1987, Gordon 1984, 1985a, 1985b, Adair and Black 2003). High discrepancies are reported even for the same strain of mice.

A major shortcoming of many experiments undertaken is the lack of well-defined exposure conditions, missing online temperature recording and poorly performed dosimetry (Repacholi 2001), which might be an explanation for the controversial results.

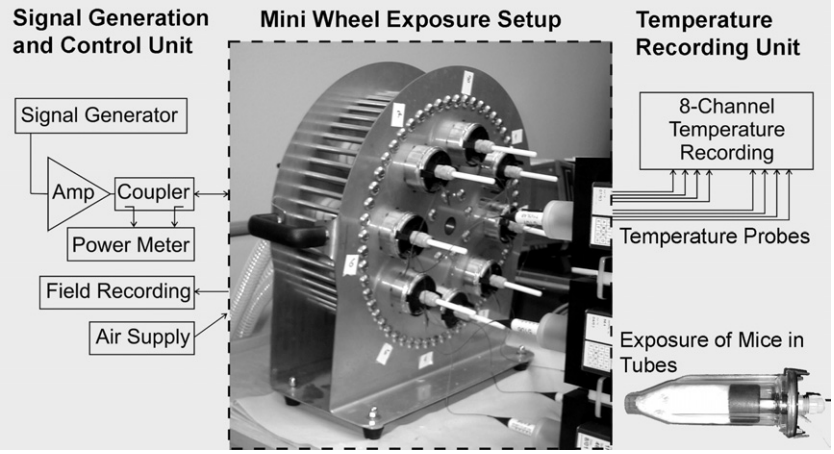

Figure 1. Mini Wheel Setup with temperature probes enabling the exposure of up to eight mice simultaneously with a 905 MHz signal. SPEAG thermistor probes enabled online high resolution body temperature measurements during the RF exposure.

The objective of this study was to assess the thermal regulatory and breakdown threshold for multiple mouse models exposed to electromagnetic fields at 905 MHz inside the setup configuration 'Ferris Wheel' which has been applied in several long- and short-term studies.

2. Material and methods

2.1. Animals

The thermal responses of the mice were examined for different body weight groups (20 g, 24 g, 29 g, 36 g), both genders (f, m), pregnant mice and two different mouse strains (B6C3F1 and NMRI). Charles River Laboratories (Sulzbach, Germany) supplied the B6C3F1 male and female mice at the ages of 4 and 12 weeks and the male NMRI mice at an age of 12 weeks. Four groups of B6C3F1 mice and one group of NMRI mice were examined. Each group consisted of at least 12 animals: eight animals used for exposure and four as sham-exposed animals. Sham-exposed animals were treated identically as exposed animals, but were not exposed to RF. The animal groups had the following parameters: group A (female B6C3F1, 20.4 ± 0.9 g, 4 weeks old), group B (female B6C3F1, 23.6 ± 0.8 g, 12 weeks old), group C (male B6C3F1, 28.8 ± 0.9 g, 12 weeks old), group D (pregnant female B6C3F1, 31 ± 2.4 g to 36 ± 3.7 g, 12 weeks old) and group E (male NMRI, 36.4 ± 3.0 g, 12 weeks old) (see also table 4).

The animals were kept in standard cages (Makrolon©, type II (350 cm^2)) in pairs or individually (only the 12-week-old males); in the cages absorbent softwood was used as bedding material. The body weight of the mice was monitored every morning. The laboratory maintained an environmental temperature of 22 ± 2 °C and a relative humidity of 30–70%. An automatic timing device provided a 12 h light/dark cycle.

2.2. Exposure protocol

Prior to the experimental period, all mice were acclimatized and trained to the restrainer tube housing required for the RF exposure (figure 1). The training also included a dummy

temperature probe. The training phase lasted for about three weeks, so that the animals had an age of 7 or 15 weeks at the start of the study. The animals were trained by increasing the amount of time spent in the tube everyday for a duration of up to 4 h. The experiment began after the training phase. Although trained identically, B6C3F1 and NMRI mice behaved differently to the tube restrained during exposure: B6C3F1 mice behaved very calmly, even partly falling asleep during the exposure. In contrast, the NMRI mice were more active and never reached the calmness of the B6C3F1 mice. The NMRI mice pawed during the entire exposure time and in rare occasions even started to hyperventilate. Due to their higher activity, a higher metabolic rate is present compared to the B6C3F1 mice.

RF exposure was performed according to a standardized exposure protocol: (1) preparation of mice with temperature probes, (2) fixation of mice in the restrainer tubes and in the exposure setup, (3) 10–20 min recording of the temperature baseline until a stable body temperature ($\Delta T < 0.1$ °C) was reached for all mice, (4) application of the RF exposure for a duration of 120 min, (5) 15–30 min recording of body temperature development after the RF exposure and (6) replacement of mice to the cages.

During the experiments, an animal caretaker was always present and a veterinarian close by. The exposure level and body temperature of the mice were monitored online, so that the safety of the animals was ensured at all times. If during the exposure the body temperature of an animal increased to more than 41 °C, the animal was replaced for safety and ethical reasons. Additionally, the exposure was interrupted if two or more animals reached 41 °C and the body temperature of the majority of the mice increased linearly to more than 40 °C.

The mouse groups were exposed to arbitrarily chosen increasing SAR levels. Groups A, C and E were exposed to sham, 2, 5, 7.2, 10, 12.6, 20 W kg^{-1} levels, group B to sham, 5, 7.2, 10, 12.6, 20 W kg^{-1} and group D to sham, 5, 10, 12.6, 20 W kg^{-1} (see also table 4). To document and monitor any environmental influences during the exposures, four additional animals of the same breed, gender and weight group were always sham exposed in a second setup.

It should be noted from the literature that an average SAR of 9.2 W kg^{-1} for a 25 g mouse corresponds to approximately the same power as the metabolic rate for a non-stressed resting female *mus musculus* mouse (Johnson *et al* 2001). Therefore, it is expected that the applied RF exposures with SAR values between 2 and 20 W kg^{-1} induce a heat load between 0.22 and 2.2 times the metabolic rate.

One exposure per mouse group per day was undertaken. Each mouse group was exposed in a series to increasing SAR levels on consecutive days at the same time slot of each day. After the series was completed, a few exposures were repeated at different times of the day to exclude any influence of the exposure time, e.g. due to the circadian temperature rhythm of the mice.

2.3. Temperature measurement

The body temperature of the mice was continuously recorded, starting at the placement of the temperature probes until the mice were taken out of the exposure setup. The temperature was recorded by rectal measurements. Eight RF-immune thermistor probes (T1V3LA, SPEAG, Switzerland) with a noise level of 0.005 °C and an absolute accuracy of 0.1 °C were continuously read in 1 s intervals by two recording systems (EASY4, SPEAG, Zurich, Switzerland). The temperatures of the four sham-exposed mice in the second setup were measured with a 4 channel temperature device (FoTemp4, OPTOCON, Germany), based on an optical measurement process (accuracy: approximately 1 °C, sample rate: 8 s).

The tip diameter of the two temperature measurement systems is 1 mm (EASY4) and 1.3 mm (FoTemp4) and allowed rectal insertion at a depth of 15 mm, as required for core body temperature measurements (Habicht 1981). Insertion accuracy during the exposure was ensured by taping the probes to the tails of the animals. During rectal measurement, the stability of the temperature was increased considerably due to mice falling asleep and/or calming down, and decreased due to mouse movement, body gases and natural body temperature drifts. For an evaluation period of 10 min, the noise level for the sham-exposed mice varied between 0.09 °C and 0.17 °C (group A: 0.12 °C, group B: 0.09 °C, group C: 0.11 °C, group D: 0.17 °C and group E: 0.13 °C).

2.4. Evaluation of thermal response

Three characteristic thermal responses of whole-body exposed mice can be distinguished (as shown in figure 3). (A) The body temperature does not change upon RF exposure, within the measurement noise limits. (B) The regulatory system of the mouse compensates the RF-induced heat load; the characteristic response was not necessarily an increase in body temperature during exposure but a decrease in body temperature after the exposure. (C) The mouse was not able to compensate the body temperature increase due to the RF; body temperature increased linearly.

Thermal regulation and breakdown were determined in the following way:

- *Regulation*: whenever the average body temperature at about 10 min after the RF exposure (evaluation period 5 min) is significantly lower (=three times the noise level) in comparison to the body temperature in the last 10 min of exposure, the mouse was regarded as being in a thermal regulatory state. The thermal regulatory threshold was set between the lowest examined SAR at which no animal showed any regulation and the lowest SAR for which at least one mouse responded.
- *Breakdown*: whenever a mouse showed a linear body temperature increase and reached temperature levels about 41 °C, it was regarded as being in the thermal breakdown region. The thermal breakdown threshold was then determined by measuring the slope of the temperature increase over time $\mathrm{d}T/\mathrm{d}t$ dependent upon the applied SAR value. Extrapolating the resulting linear regression curve to $\mathrm{d}T/\mathrm{d}t = 0$ reveals a SAR value which was used as the breakdown threshold.

2.5. Radiofrequency exposure

The mice were exposed inside a 'Mini Wheel Setup', the concept of which was derived from the 'Ferris Wheel Setup' (Balzano *et al* 2000). The Mini Wheel Setup has a mono-mode cavity and therefore well-defined exposure conditions (cavity diameter 332 mm, plate separation 120 mm). The setup enables the exposure of up to eight mice simultaneously and is designed as a resonant waveguide structure of two parallel, circularly shaped metallic plates shorted with metallic bars along the outer edge and with an isotropic antenna at the centre. The mice were circularly positioned in restrainer tubes at a fixed radial distance of 111.5 mm from the antenna with the animal body axis orientated parallel to the E-field. The system was matched for resonance (return loss $\leqslant -18$ dB) using a triple stub tuner (Type 1878B, Maury Microwave, USA). An air ventilation system forced a constant airflow of about 1 l min^{-1} (measured in empty tubes) through the tubes. This ensured sufficient fresh air for the mice while restrained in the one-size tubes and lead to about the same airflow through the tubes for all mice, regardless of their size. RF signals were generated by a signal generator (SMIQ 02B, Rohde&Schwarz, Germany) and an amplifier (model 2449R2, LS Elektronik, Sweden). For

exposure control, the forward and reflected powers as well as the electric field inside the cavity were measured. Power measurements were performed with a dual directional coupler (Type 778D, Hewlett Packard, USA) and a dual head power meter (E4419B EPM, Agilent, USA). The incident E-field measurement inside the wheel was performed by two monopole sensors (length = 10.5 mm; at a radius of 20 mm) connected to diode detectors (ACSP2663NZC15, Advanced Control Components, USA).

A detailed numerical and experimental dosimetry and a comprehensive uncertainty assessment of the Mini Wheel Setup were performed. The uncertainty budget was assessed according to Taylor and Kuyatt (1994), taking all the occurring variabilities and variations into account. The numerical dosimetry is based on FDTD simulations (using SEMCAD 1.8, SPEAG, Switzerland) with high resolution mouse models for different animal sizes (scaled models corresponding to mouse weights of 20 g, 25 g, 30 g, 35 g) and postures (restrained and non-restrained mouse in tube). The mouse models were derived from Microtom slices of 1 mm resolution. The numerical examination included simulations of the full exposure setup filled with eight mice as well as simulations in a one and three mouse sector model. The experimental dosimetry used mouse dummies (conical bottles filled with tissue simulating liquid) to assess the dependence of the exposure on the eight positions within the wheel and to verify the numerical FDTD model by precise E-field using a near-field scanner (DASY4, SPEAG, Switzerland) and temperature measurements. Examinations were performed on the influence of various parameters on SAR as listed in tables 2 and 3. In addition to the whole-body SAR assessment, detailed organ/tissue specific SAR values were determined as shown in table 1.

An uncertainty assessment for the whole-body and organ averaged SAR was performed according to Kuster *et al* (2005). The uncertainty budget includes the absolute uncertainties of the SAR assessment and the variabilities of SAR between different mice in the setup and due to mice movement. The uncertainty of the SAR assessment of the whole-body averaged SAR was estimated to be ± 1.2 dB ($\pm 33\%$, $K = 1$) (see also table 2). Variations in SAR during the experiment including movements, position within the wheel, posture, etc were estimated to be ± 1.1 dB ($\pm 27\%$, $K = 1$) for the whole-body averaged SAR (table 3).

With respect to thermosensitivity and thermoregulatory responses, organs with thermal receptors are of interest, such as the hypothalamus in the brain and the skin (Ahlbom *et al* 1998). The averaged tissue specific SAR of the brain is -1.1 dB (-23%) less in relation to the whole-body averaged SAR; the exposure of the skin in relation to the whole-body averaged SAR was about 2.6 dB (80%) higher (table 1). However, a higher local exposure in SAR does not necessarily lead to a higher local temperature; blood flow etc can distribute the heat rapidly. Figure 2 shows the SAR distribution in a centre sagittal section of the mouse model in a tube.

3. Results

Figure 3 shows the measured characteristic thermal response curves for below, in and above the regulatory region. Table 4 summarizes the results for the different mouse groups and exposure strengths. All mice were evaluated individually. Listed are the amounts of particular mice out of the total number of mice which reached either the thermal regulatory or the breakdown region at the various exposure levels. No thermal regulation in any mouse was observed at an exposure level of 2 W kg^{-1}. Thermal response was measured starting at 5 W kg^{-1}.

Figure 4 shows the detailed evaluation of the breakdown threshold. Plotted is the temperature increase per time of all mice in the thermal breakdown range as a function of the applied SAR. The linear regression for each data point was used to extrapolate the lowest

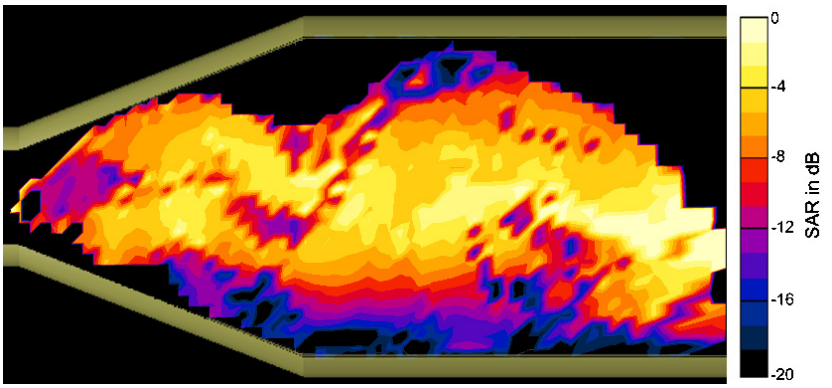

Figure 2. SAR distribution in the centre sagittal cut through a 25 g high-resolution mouse model (0 dB equals 0.07 W kg^{-1}).

(This figure is in colour only in the electronic version)

Table 1. Simulated SAR for specific organs/tissues.

Organ/Tissue type	Organ/tissue deviation[a] (dB)	Uniformity[b] (dB)	Isotropy[c] (dB)
Whole-body	0.00	5.29	0.19
Avg. brain	−1.14	−4.88	0.40
Avg. muscle	0.88	5.23	0.20
Bladder	0.97	−4.35	0.81
Blood	1.90	−3.12	0.26
Bone (cortical)	−2.46	4.79	0.30
Bone marrow (infiltrated)	−7.21	−2.04	0.34
Cartilage	−1.46	−0.96	1.23
Cerebrospinal fluid	2.80	0.29	1.12
Eye tissues (sclera)	0.54	−4.65	0.62
Fat (averaged infiltrated)	−5.16	4.80	0.48
Heart	−0.59	−4.23	0.77
Kidney	−1.76	−3.33	1.00
Liver	−1.43	−2.90	0.21
Lung (deflated)	−1.08	−4.81	0.83
Nerve	−1.04	−2.15	0.26
Skin (wet)	2.56	7.59	0.67
Small intestine	1.99	−0.56	0.53
Spleen	−4.59	−3.85	1.76
Stomach	−2.11	−3.10	1.11
Testis	1.78	−0.11	0.84
Tongue	0.57	−5.93	0.28
Trachea	1.35	−5.38	0.46
Vitreous humor	1.72	−4.72	0.25

[a] Organ/tissue deviation: ratio in dB of organ/tissue averaged SAR to whole-body averaged SAR.
[b] Uniformity: ratio in dB of the standard deviation of the organ/tissue averaged SAR to the organ/tissue averaged SAR to the organ/tissue averaged SAR.
[c] Isotropy: standard deviation in dB of the organ/tissue averaged SAR for the different positions in the wheel.

Table 2. Uncertainty assessment of the whole-body averaged SAR.

Error description	Tolerance (dB)	Probability distribution	Div	c_i	Uncertainty (dB)
Setup model[a]	0.94	Normal	1.0	1.0	0.94
Transfer calibration					
Calibration of reference probe	0.42	Normal	1.0	1.0	0.42
Position of reference probe (±1 mm)	0.61	Rectangular	$\sqrt{3}$	1.0	0.35
Load dependence of field transformation	0.61	Rectangular	$\sqrt{3}$	1.0	0.35
Probe linearity	0.10	Rectangular	$\sqrt{3}$	1.0	0.06
Accuracy of data logger	0.00	Normal	1.0	1.0	0.00
Mouse model					
Anatomy[b]	0.29	Rectangular	$\sqrt{3}$	1.0	0.17
Discretization (reference $(0.5\ \text{mm})^3$)[c]	0.61	Rectangular	$\sqrt{3}$	1.0	0.35
Conductivity ($\Delta\sigma = \pm 10\%$)[d]	0.15	Rectangular	$\sqrt{3}$	1.0	0.08
Permitivity ($\Delta\epsilon = \pm 10\%$)[d]	0.24	Rectangular	$\sqrt{3}$	1.0	0.14
Combined standard uncertainty					1.22
Combined extended uncertainty ($K = 2$)					2.44

[a] Deviation between measurements with dummies and simulations.
[b] Deviation due to segmentation of the mouse model and for different strains.
[c] Deviations of SAR between the applied FDTD voxel size of $(0.5\ \text{mm})^3$ and the reference model with a $(0.2\ \text{mm})^3$ resolution (determined for a plane wave exposure).
[d] Uncertainty in SAR for the deviation of the used tissue conductivity and permitivity compared to real parameters. This value was assessed by varying the tissue parameters.

Table 3. Estimation of the whole-body SAR variations.

Error description	Tolerance (dB)	Probability distribution	Div	c_i	Uncertainty (dB)
Power drift during exposure	0.15	Rectangular	$\sqrt{3}$	1.0	0.09
Isotropy within the setup[a]	0.20	Rectangular	$\sqrt{3}$	1.0	0.12
Deviations due to unbalanced loading[b]	0.79	Rectangular	$\sqrt{3}$	1.0	0.46
Variations in anatomy besides size	1.30	Rectangular	$\sqrt{3}$	1.0	0.75
Skin parameters (dry versus wet)	0.04	Rectangular	$\sqrt{3}$	1.0	0.02
Varying mouse postures[c]	0.94	Rectangular	$\sqrt{3}$	1.0	0.54
Fit function for different mouse weights[d]	0.01	Normal	1.0	1.0	0.01
Mouse movements					
Shift in x-direction (±2 mm)	0.13	Rectangular	$\sqrt{3}$	1.0	0.08
Shift in y-direction (±2 mm)	0.11	Rectangular	$\sqrt{3}$	1.0	0.06
Shift along body axis (z-direction) (±5 mm)	0.24	Rectangular	$\sqrt{3}$	1.0	0.14
Combined standard uncertainty					1.06
Combined extended uncertainty ($K = 2$)					2.12

[a] Isotropy in SAR within the setup loaded with reference dummies.
[b] Deviation of SAR for a 20% lighter dummy between averaged weight reference dummies.
[c] Deviation in SAR for stuffed versus non-stuffed mouse model.
[d] Averaged deviation for fit function SAR(m) with m as mouse weight while using scaled mice models.

SAR value for thermal breakdown ($dT/dt = 0$). A value of $10.1 \pm 4.0\ \text{W kg}^{-1} (K = 2)$ for B6C3F1 mice and $7.7 \pm 1.6\ \text{W kg}^{-1} (K = 2)$ for NMRI mice was found (the variations correspond to the standard deviation of the fit multiplied with the factor $K = 2$ according to Taylor and Kuyatt (1994)).

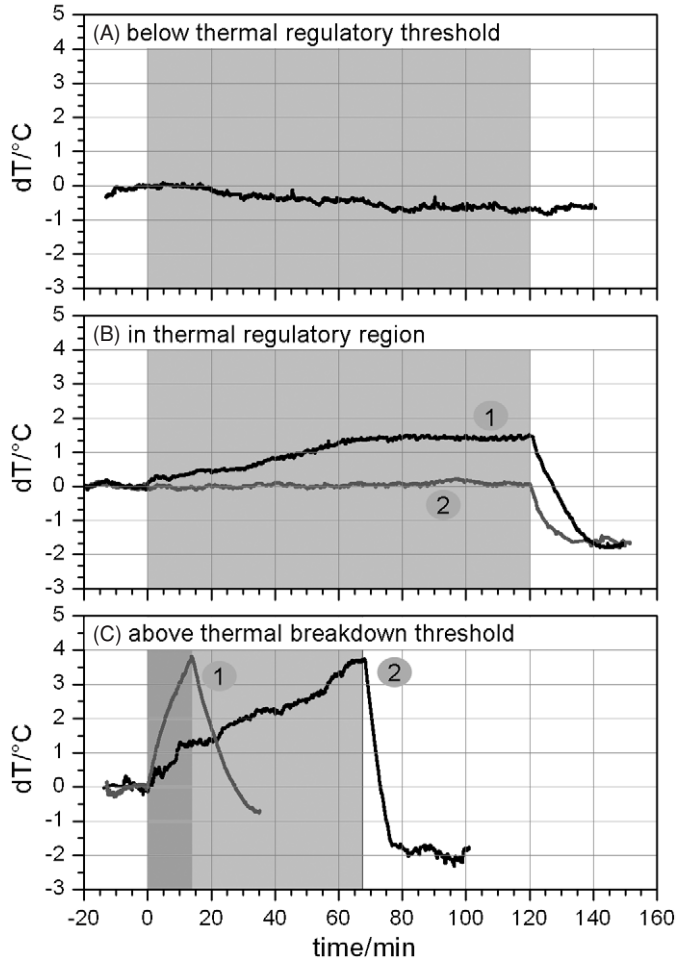

Figure 3. Characteristic thermal response curves for below, in and above the regulatory region. The RF on phase is marked as a grey background. Part (A) shows the thermal response of a mouse exposed to a SAR below the thermal threshold (no increase in temperature). Part (B) shows the two cases in the regulatory region: (1) an increase in body temperature occurs, but stabilizes at a higher level and (2) no temperature increase is measurable during exposure, but after the exposure was switched off. Part (C) shows two thermal responses above the breakdown threshold for different SAR levels: (1) at SAR = 20 W kg^{-1} and (2) at SAR = 12.6 W kg^{-1}.

No recognizable differences between the additional four sham-exposed animals on any exposure day were observed. No influence from the exposure time slot was observed when exposures were repeated at different times of the day.

When comparing the individual mouse groups, further observations regarding the different behaviour with respect to weight classes, gender, pregnancy and strains can be made: (1) weight classes: by comparing the number of animals with thermal responses across the groups A to D, representing increasing body weights, the thermal response in mice increases with increasing body weight. (2) Gender: when comparing the different genders of groups B and C, male mice seem more sensitive to the RF-induced heat load: a higher number of animals responded in the thermal regulatory as well as breakdown regions. Also when compared to the heavier females

Table 4. The upper part of the table lists the five examined mouse groups. The middle part shows the number of animals out of the total number of animals exposed which reached the thermal regulatory threshold. The lower part shows the number of animals which reached the thermal breakdown threshold.

Group	Gender	Type	Mass (g)	Age at delivery (weeks)
		Exposure groups		
A	Female	B6C3F1	20.4 ± 0.9	4
B	Female	B6C3F1	23.6 ± 0.8	12
C	Male	B6C3F1	28.8 ± 0.9	12
D	Pregnant female	B6C3F1	31 ± 2.4 to 36 ± 3.7	12
E	Male	NMRI	36.4 ± 3.0	12
Group	2 W kg^{-1} (# Animals)	5 W kg^{-1} (# Animals)	7.2 W kg^{-1} (# Animals)	10 W kg^{-1} (# Animals)
		Thermal regulatory threshold		
A	0/8	1/8	5/8	6/8
B	-/-	4/8	6/8	8/8
C	0/8	7/8	8/8	8/8
D	-/-	4/8	-/-	7/8
E	0/8	8/8	8/8	8/8
Group	7.2 W kg^{-1} (# Animals)	10 W kg^{-1} (# Animals)	12.6 W kg^{-1} (# Animals)	20 W kg^{-1} (# Animals)
		Thermal breakdown threshold		
A	0/8	0/8	4/8	7/8
B	0/8	0/8	4/8	8/8
C	0/8	1/8	7/8	8/8
D	-/-	5/8	6/8	8/8
E	0/8	2/8	8/8	8/8

of group D, more male animals of group C responded to the RF in the thermal regulating region, although fewer male animals responded in the breakdown region. However, gender specific responses might be due to the effect of a higher body mass and/or different metabolic rates between the groups. (3) Influence on pregnancy: the pregnant mice of group D responded to the RF exposure with a similar thermal regulatory response as the non-pregnant mice (group B). Slight differences were observed for the breakdown threshold, which is by about 1 W kg^{-1} below the non-pregnant animals. This may also be an effect from the higher body mass and/or different metabolic rates of the pregnant mice. (4) Strain: the NMRI mice show a different thermal response when compared to B6C3F1: more animals responded with thermal regulation at the same SAR level, and the breakdown threshold is reached significantly earlier, already at 7.7 W kg^{-1} versus 9.7–10.8 W kg^{-1} for B6C3F1. However, the differences may also be due to the different body masses and metabolic rates.

4. Discussion

The results indicate that the metabolic rate is an important factor for the thermal response: the literature describes the basal metabolic rate of a mouse (approximately 0.3 W for a 30 g mouse) as being dependent upon the body mass according to the relationship m^x with $0.7 < x < 0.8$

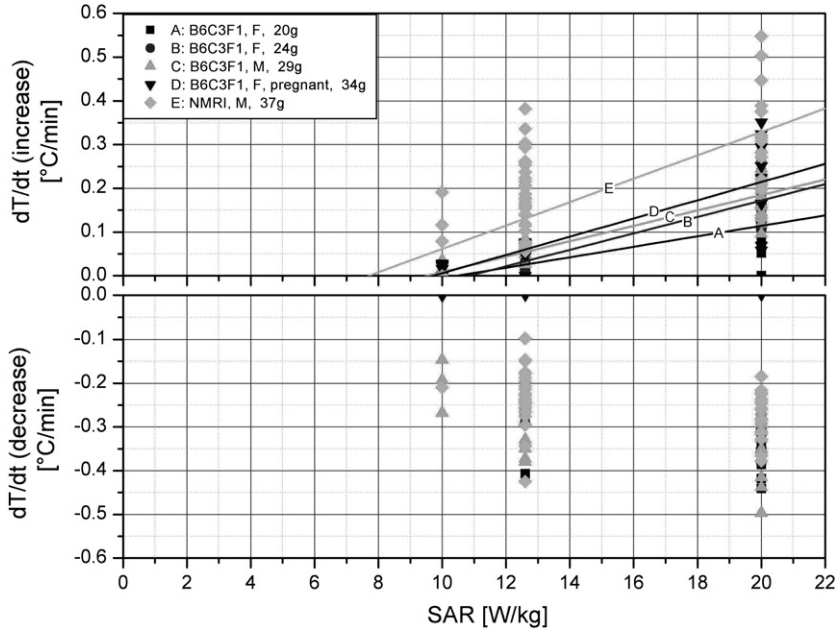

Figure 4. Linear body heat storage increase/decrease rate for different SAR levels in the breakdown region. Each marker represents the slope of the linear body temperature change in one mouse at the exposed SAR level. The linear regression fits were evaluated for each exposure group. The thermal breakdown threshold corresponds to the SAR level with no heat storage change (group A: 10.5 ± 1.0 W kg^{-1}, group B: 10.8 ± 0.6 W kg^{-1}, group C: 9.5 ± 0.4 W kg^{-1}, group D: 9.7 ± 1.6 W kg^{-1} and group E: 7.7 ± 0.8 W kg^{-1}). The averaged thermal breakdown threshold is 7.7 ± 0.8 W kg^{-1} for NMRI mice and 10.1 ± 2.0 W kg^{-1} for B6C3F1 mice. Mice are able to cool with a rate of approximately 0.3 °C min^{-1} after RF is switched off.

(Porter 2001, Dodds *et al* 2001, Johnson *et al* 2001). Right below the thermal breakdown threshold in the temperature steady state, the cooling capacity is working at its limit. The threshold SAR is then directly connected to the metabolic rate. The power from metabolic processes and RF absorption must equalize with the cooling rate $M + P_{RF} = C$ (derived from equation (1)). For example, assuming a 30 g mouse with a basal metabolic rate of 0.3 W, the cooling rate becomes $C = 0.6$ W when exposed to 10 W kg^{-1}, which is twice as high as the basal metabolic rate.

Since the maximal cooling capacity is constant, higher metabolic rates lead to increased temperature responses and therefore a lower thermal breakdown threshold. If the heat balance equation also takes into account additional heat sources like muscle movements or stress, the thermal breakdown threshold is further reduced. This is manifested by the observed lowered threshold with increasing mass or increased stress level of the NMRI mice. Furthermore, the results indicate that animals with excessive weight seem more sensitive for the same SAR level.

The threshold for the thermal regulatory response is more difficult to assess. However, the current data suggest a threshold between 2 and 5 W kg^{-1}, which is very close to the thermal breakdown level, with a lower limit of 6 W kg^{-1} ($K = 2$). It should be noted that the presented results were obtained for whole-body exposure of restrained mice in tubes (as applied in several risk assessment studies), where the heat transfer is different when compared to free running animals (see also equation (1)). However, the determined threshold values are

close to those on which the current safety standards (Ahlbom *et al* 1998) are based, which rely on a thermal threshold value of 4 W kg^{-1} for adverse health effects. Further examination and precise determination of the thresholds, e.g. also for different species, seem necessary.

In general, the data of our study are also in line with the results of Lu *et al* (1987), who derived a thermal regulatory threshold of 2 W kg^{-1} in different strains of rats (exposed to a 120 Hz modulated 2.45 GHz signal for 2 h). Lu further determined a breakdown threshold of 9.2–11.5 W kg^{-1}. Additionally, disruption of food-motivated learning behaviour was found to occur between 3 and 9 W kg^{-1} across a number of animal species and frequencies (Osepchuk and Petersen 2003). However, the uncertainties of the dosimetry for these studies are not provided and are difficult to estimate.

5. Conclusion

Three characteristic thermal responses were identified: (1) no thermal regulation, (2) response of the thermal regulatory system capable of compensating the RF-induced temperature load and (3) thermal breakdown, i.e., uncompensated body temperature increase. No thermal regulation was measured for exposure levels of 2 W kg^{-1}. Thermal regulation was observed at 5 W kg^{-1}. The thermal breakdown threshold was determined to be 10.1 ± 4.0 W kg^{-1}($K = 2$) for B6C3F1 mice and 7.7 ± 1.6 W kg^{-1}($K = 2$) for NMRI mice. The thermal response was found to be dependent upon the metabolic rate of the animal, which is a function of body mass and also depends on the activity level. The presented data suggest that the thermal breakdown for in-tube restrained mice, whole-body exposed to RF, may occur at SAR levels of 6 W kg^{-1} ($K = 2$) at laboratory conditions. Considering the uncertainty of the SAR assessment, the minimal level might even be below this threshold. Furthermore, it is expected that the threshold is higher for free-running animals at the same conditions and lower for restrained animals at higher environment temperatures.

Acknowledgments

This study was supported by the Fraunhofer Institute for Toxicology and Experimental Medicine (Germany) and TDC Sunrise (Switzerland).

References

Adair E R, Adams B W and Hartman S K 1992 Physiological interaction processes and radiofrequency energy-absorption *Bioelectromagnetics* **13** 497–512

Adair E R, Adams B W and Kelleher S A 1993 Resonant CW and pulsed fields of identical average power densities provoke similar thermoregulatory adjustments by squirrel monkeys *BEMS 15th Annual Meeting Abstract Book* p 63

Adair E R and Black D R 2003 Thermoregulatory responses to RF energy absorption *Bioelectromagnetics* (Suppl 6) S17–38

Ahlbom A *et al* 1998 Guidelines for limiting exposure to time-varying electric, magnetic, and electromagnetic fields (up to 300 GHz) *Health Phys.* **74** 494–522

Balzano Q, Chou C K, Cicchetti R, Faraone A and Tay R Y S 2000 An efficient RF exposure system with precise whole-body average SAR determination for *in vivo* animal studies at 900 MHz *IEEE Trans. Microwave Theory Tech.* **48** 2040–9

Dodds P S, Rothman D H and Weitz J S 2001 Re-examination of the '3/4-law' of metabolism *J. Theor. Biol.* **209** 9–27

Gordon C J 1982 Effect of heating rate on evaporative heat loss in the microwave-exposed mouse *J. Am. Physiol. Soc.*

Gordon C J 1983a Behavioral and autonomic thermoregulation in mice exposed to microwave-radiation *J. Appl. Physiol.* **55** 1242–8

Gordon C J 1983b Influence of heating rate on control of heat-loss from the tail in mice *Am. J. Physiol.* **244** R778–84
Gordon C J 1984 Relationship between autonomic and behavioral thermoregulation in the mouse *Physiol. Behav.* **34** 687–90
Gordon C J 1985a Body temperature in the mouse, hamster, and rat exposed to radiofrequency radiation: an interspecies comparison *J. Thermical. Biol.*
Gordon C J 1985b Temperature regulation in the mouse and hamster exposed to microwaves in hot environment *Health Phys.*
Gordon C J and White E C 1982 Distinction between heating rate and total heat absorption in the microwave-exposed mouse *Physiol. Zool.* **55** 300–8
Habicht G S 1981 Body temperature in normal and endotoxin-treated mice of different ages *Mech. Ageing Dev.* **16** 97–104
Johnson M S, Thomson S C and Speakman J R 2001 Limits to sustained energy intake II. Inter-relationships between resting metabolic rate, life-history traits and morphology in mus musculus *J. Exp. Biol.* **204** 1937–46
Kuster N, Berdinas T V and Nikoloski N 2005 Methodology of detailed dosimetry and treatment of uncertainty and variations for *in vivo* studies *Bioelectromagnetics* submitted
Kuster N and Schonborn F 2000 Recommended minimal requirements and development guidelines for exposure setups of bio-experiments addressing the health risk concern of wireless communications *Bioelectromagnetics* **21** 508–14
Lu S-T, Lebda N A, Lu S-J, Pettit S and Michaelson S M 1987 Effects of microwaves on three different strains of rats *Radiat.-Res.* **110** 173–91
Osepchuk J M and Petersen R C 2003 Historical review of RF exposure standards and the International Committee on Electromagnetic Safety (ICES) *Bioelectromagnetics* (Suppl 6) S7–16
Porter R K 2001 Allometry of mammalian cellular oxygen consumption *Cell. Mol. Life Sci.* **58** 815–22
Repacholi M H 2001 Health risks from the use of mobile phones *Toxicol. Lett.* **120** 323–31
Taylor B N and Kuyatt C E 1994 Guidelines for evaluating and expressing the uncertainty of NIST measurement results *Nat. Inst. Stand. & Technol. (Washington, DC)* p 26